



Research article

UDC 624.01

DOI: 10.34910/MCE.127.2



## Mechanical behavior and eco-efficiency of sisal fiber reinforced cement composites containing husk rice ash

K.G. Calazans<sup>1</sup> , P.R.L. Lima<sup>1</sup>  , R.D. Toledo Filho<sup>2</sup> 

<sup>1</sup> State University of Feira de Santana, Bahia, Brazil

<sup>2</sup> Federal University of Rio de Janeiro, Rio de Janeiro, Brazil

 [prllima@uefs.br](mailto:prllima@uefs.br)

**Keywords:** fiber cement composites, rice husk ash, CO<sub>2</sub> emission, mechanical behavior, eco-strength efficiency, embodied energy

**Abstract.** The use of cementitious composites reinforced with plant fibers in construction elements has emerged as a promising alternative to mitigate the environmental impact of the construction industry. The challenge of chemical incompatibility between plant fibers and the matrix has been addressed through the incorporation of mineral additives, with metakaolin being the most commonly used despite its high energy consumption during production and CO<sub>2</sub> generation. An alternative to this industrial additive is rice husk ash (RHA), a pozzolanic material derived from agricultural waste. The research aims to evaluate the influence of a high RHA content replacing cement on the mechanical properties and sustainability indicators of composites reinforced with 4 % and 6 %, by mass, of sisal fibers. Composites incorporating 50 % RHA exhibited higher compressive strength, multiple cracks, and increased toughness under flexion compared to composites with metakaolin, fly ash, and silica of fume. Sustainability assessments indicated that replacing metakaolin with RHA resulted in reduced CO<sub>2</sub> emissions and embodied energy, contributing to the enhanced eco-efficiency of the composites. This improvement was particularly notable in terms of increased compressive strength and toughness.

**Funding:** CNPq (Grant number 102164/2022- 4363)

**Citation:** Calazans, K.G., Lima, P.R.L., Toledo Filho, R.D. Mechanical behavior and eco-efficiency of sisal fiber reinforced cement composites containing husk rice ash. Magazine of Civil Engineering. 2024. 17(3). Article no. 12702. DOI: 10.34910/MCE.127.2

### 1. Introduction

One of the primary challenges in civil construction is aligning with the United Nations' Sustainable Development Goals, particularly in the context of establishing inclusive, sustainable, and resilient cities. To attain this objective, a pivotal step for civil engineering is the utilization of sustainable materials that not only curtail greenhouse gas emissions but also exhibit lower energy consumption during their production. In this context, the incorporation of waste materials from other industrial sectors into the construction industry offers an advantage over traditional materials because they are ready for use after minimal processing operations, which have a lower environmental impact. In the case of utilizing agro-industrial waste, such as rice husk, there is an added benefit of it originating from plant sources that sequester carbon during their growth, thus contributing to minimizing environmental harm caused by transformation processes required to make them suitable for construction materials.

Rice husk ash (RHA) has emerged as a promising mineral addition in cement-based material production [1], offering various benefits that enhance the sustainability and performance of construction materials. In recent years, several studies have demonstrated the positive effects of incorporating RHA in

concrete, leading to increased compressive strength, improved durability, and a reduced environmental impact in the construction industry. It can be used in the production of normal concrete [2], contributing to the widespread use of this sustainable additive in standard construction practices. Additionally, RHA has shown promise in producing lightweight concrete for use in bricks [3], concrete containing recycled aggregates [4], and self-compacting concrete for highway pavements [5]. By replacing a portion of cement with RHA, the construction industry can significantly enhance its sustainability profile, since cement production is a major contributor to greenhouse gases emissions and energy consumption in the civil construction sector. Therefore, integrating RHA into concrete formulations helps mitigate the environmental impact, reduce CO<sub>2</sub> emissions, and conserve energy resources, contributing to a greener and more eco-friendly construction sector.

The utilization of RHA in cementitious matrices for cement-based composites reinforced with plant fibers was initially explored in the 1980s, with researchers studying its potential benefits [6–8]. The natural fiber reinforced cement composites offer the opportunity to produce robust and durable construction elements, suitable for various applications, such as blocks for precast slabs [9], sandwich panels [10], lightweight tiles, which enhance the thermal comfort of buildings in urban and rural areas [11] or ultra-high-performance concrete [12]. Plant fibers, being renewable resources, hold a sustainability advantage over steel and polymeric fibers. However, their successful application as reinforcement in cement-based composites requires overcoming the potential chemical incompatibility between the fibers and the hydrated cement compounds. To address this, two main approaches have been employed by researchers: application of chemical treatment to the fiber [13] or developing calcium hydroxide-free (CH-free) matrices, which are responsible for a mineralization process of the vegetable fiber [14].

To create CH-free cementitious matrices, researchers have successfully replaced a portion of the cement with mineral additions that exhibit excellent pozzolanic reactivity. These mineral additions, such as fly ash, silica of fume, and metakaolinite, react with calcium hydroxide produced during cement hydration to form additional cementitious compounds. This process not only improves the strength and durability of the cementitious matrix but also reduces the potential for chemical incompatibility with vegetable fibers [14]. Despite the advantages of using RHA as a mineral addition to improve cement-based composites reinforced with plant fibers [15], the development of constructive elements using these materials has primarily employed silica of fume [9] or metakaolinite [10].

Certainly, rice husk ash offers numerous advantages over industrial mineral additions like metakaolinite, particularly in terms of enhancing sustainability in construction materials. RHA is a byproduct obtained from the combustion of plant biomass, making it both renewable and readily available. For use in construction, RHA undergoes a grinding and drying process, resulting in equivalent CO<sub>2</sub> emissions ranging from 103.2 to 157 kg CO<sub>2</sub>/t [16, 17], as well as energy consumption in the range of 200 to 2070 MJ/t [17–19]. In contrast, industrial mineral additives, such as metakaolinite, are manufactured using energy-intensive processes and are non-renewable, resulting in a greater environmental impact and depletion of finite resources. The substantial equivalent CO<sub>2</sub> emissions associated with metakaolinite, which can vary from 236 to 840 kg CO<sub>2</sub>/t [16, 20–22], stem from the energy-intensive processes, with energy consumption ranging from 2720 to 3300 MJ/t [18, 23]. These processes involve calcination and grinding operations during its production. Despite this environmental impact, metakaolin is extensively used due to its ability to enhance mechanical strength. This highlights the need for studies that assess the relationship between mechanical efficiency and sustainability, as will be presented in this article.

The aim of this study is to perform a comparative analysis of the influence of various mineral additions, used as substitutes for cement, on the mechanical properties and sustainability of sisal fiber reinforced cement composites (SFRCC). To achieve this, SFRCC were produced and reinforced with 4 % and 6 %, in mass, of sisal fiber, incorporating rice husk ash, metakaolinite, fly ash, and silica of fume. They were then subjected to direct compression and bending tests. Additionally, this research assesses the CO<sub>2</sub> emissions, energy consumption, and eco-efficiency of composites reinforced with 4 % sisal fibers.

## 2. *Materials and Methods*

### 2.1. *Materials*

The sisal fibers were sourced from Valente, Brazil. A pre-treatment procedure involved immersing the fibers in water at 50° C for 1 hour to eliminate residues adhering to their surface. Following this, the fibers were manually aligned and cut to a length of 40 mm. An alkaline treatment based on calcium hydroxide was applied to the fibers in order to improve their adhesion with the matrix. The procedure was performed with immersion of the fibers in a solution of calcium hydroxide – Ca(OH)<sub>2</sub>, at a concentration of 0.73 %. After 50 minutes of immersion, the fibers were removed, placed in sieves for drying in the open air. After treatment, the fibers showed a lower rate of water absorption and higher tensile strength, comparative to natural fibers.

To produce the cementitious matrix of the composites, natural quartz sand with particles smaller than 600  $\mu\text{m}$  and density of 2.67  $\text{g}/\text{cm}^3$  was used. The binder was formed by a combination of high initial strength Portland cement, metakalonite (MK), silica, fly ash, and rice husk ash. The rice husk ash used in this work, commercially known as amorphous rice husk silica (SILCCA NOBRE), is produced by controlled combustion via fluidized bed of rice husk agricultural waste from the food industry. The chemical composition and density of these materials is shown in Table 1 while in Fig. 1 the particle size curves are shown.

According to ASTM C618, all binders can be classified as pozzolanic material since the sum of three oxides from their chemical analyses,  $\text{SiO}_2 + \text{Al}_2\text{O}_3 + \text{Fe}_2\text{O}_3$ , was higher than 70 %. The granulometry of the binders, represented in Table 1 by the D50 diameter, corresponding to cumulative passing at 50 %, confirms that the rice husk ash has a fineness compatible with cement and metakaolinite, which enhances its chemical reactivity.

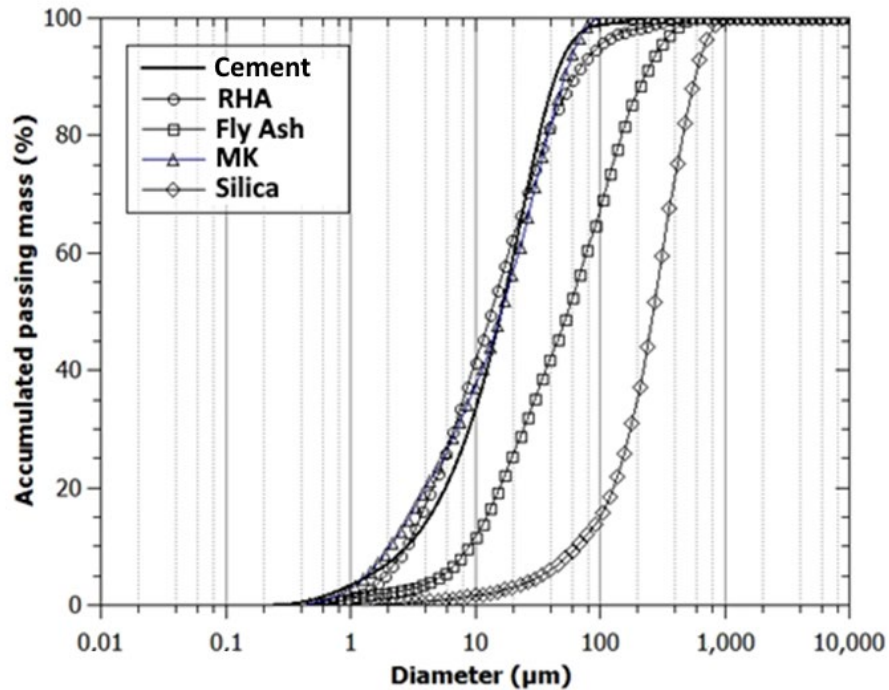


Figure 1. Granulometric curves of binders.

Table 1. Chemical composition, density and medium diameter of binders.

Major chemical component (%)	Cement	Fly ash (FA)	Silica of fume (SF)	Rice husk ash (RHA)	Metakaolin
CaO	68.97	1.94	0.52	0.78	–
SiO <sub>2</sub>	14.95	52.24	94.90	94.95	51.85
Al <sub>2</sub> O <sub>3</sub>	4.70	33.80	1.91	–	41.69
SO <sub>3</sub>	4.29	1.79	1.59	1.25	1.09
Fe <sub>2</sub> O <sub>3</sub>	3.50	4.91	0.10	0.07	1.91
K <sub>2</sub> O	0.98	3.44	0.86	2.37	1.89
Density ( $\text{g}/\text{cm}^3$ )	3.18	2.16	2.39	2.24	2.81
D50 ( $\mu\text{m}$ )	17.4	60.2	275.4	15.1	17.4

The cement matrices, in the proportion of 1 : 1 : 0.5 (binder : sand : water/binder ratio, by weight), were prepared with the use of different binders in three combinations, as shown in Table 2. The cement content was 50 % of the total mass of binder in all mixtures. The mix 30MK has, in addition to cement, 30 % metakaolinite ash, 10 % fly ash, and 10 % silica of fume. The mix 30RHA had the objective of evaluating the replacement of metakaolinite by 30 % of the rice husk ash, keeping the cement and the other mineral additions. The mix 50RHA replaces all mineral additions with rice husk ash; the binder being made up of 50 % cement and 50 % rice husk ash. With these three matrices, SFRCC were produced with the addition of 4 % and 6 %, by mass, of sisal fiber randomly distributed in the mixture.

**Table 2. Mix proportions of the composites (kg/m<sup>3</sup>).**

Components		30MK4%	30RHA4%	30RHA6%	50RHA4%	50RHA6%
Binder	Cement	389.4	381.4	374.3	381.1	374.0
	Metakaolin	233.7	–	–	–	–
	Rice husk ash	–	228.8	224.6	381.1	374.0
	Fly ash	77.9	76.3	74.9	–	–
	Silica of fume	77.9	76.3	74.9	–	–
Aggregate	Sand	778.9	762.8	748.6	762.2	748.0
Additives	Plasticizer	7.8	7.6	7.5	7.6	7.5
	Viscosity agent	3.9	3.8	3.7	3.8	3.7
Water		389.4	381.4	374.3	381.1	374.0
Fiber		31.1	30.5	44.9	30.5	44.9

## 2.2. Methods

A third-generation superplasticizer with a solid content of 31 % and density of 1.06 g/cm<sup>3</sup> was added to the mixtures to ensure a self-compacting behavior for all matrices. The viscosity modifier admixture Rheomac UW 410, with density of 0.7 g/cm<sup>3</sup>, at a dosage of 0.05 % relative to the binder, by mass, was also used to avoid segregation of composites during molding. The composites were produced in a bench mortar with a capacity of 20 dm<sup>3</sup> and their flowability was tested using a flow table.

The uniaxial compression test was carried out on a 100 kN Shimadzu machine at a rate of axial displacement of 0.2 mm/min. The static-elastic chord modulus of elasticity was calculated from the stress-strain diagram, as recommended by ASTM C 469.

For the 4-point bending test, three plates were cut in prismatic specimens with dimensions of 400 mm × 80 mm × 15 mm and tested over a span of 300 mm at a displacement rate of 0.3 mm/min with a 100 kN Shimadzu machine, with the load cell of 1 kN. From the load–deflection curves three parameters were calculated to evaluate the fiber reinforcement effect: a) the first-cracking flexural stress ( $\sigma_{fc}$ ), determined from the load correspondent to first crack; b) the maximum stress post-cracking of the composite ( $\sigma_{pc}$ ), determined from the maximum load supported by the composite after the first crack; and c) the toughness, defined as the area under stress–deflection curves. The evaluation of the cracking pattern was performed through the analysis of images obtained from different displacement stages. A CANON D90 digital camera with Macro Lens and 10 megapixel resolution was used, which captured high resolution images every 30 seconds.

## 3. Results and Discussion

### 3.1. Mechanical behaviour of SFRCC

#### 3.3.1. Mechanical behavior under compression

Fig. 2 illustrates typical stress-strain curves for the composites under compression at curing times of 7, 28, and 56 days. The curves allowed us to determine the compressive strength values, corresponding to the maximum tension reached during the test, and the modulus of elasticity.

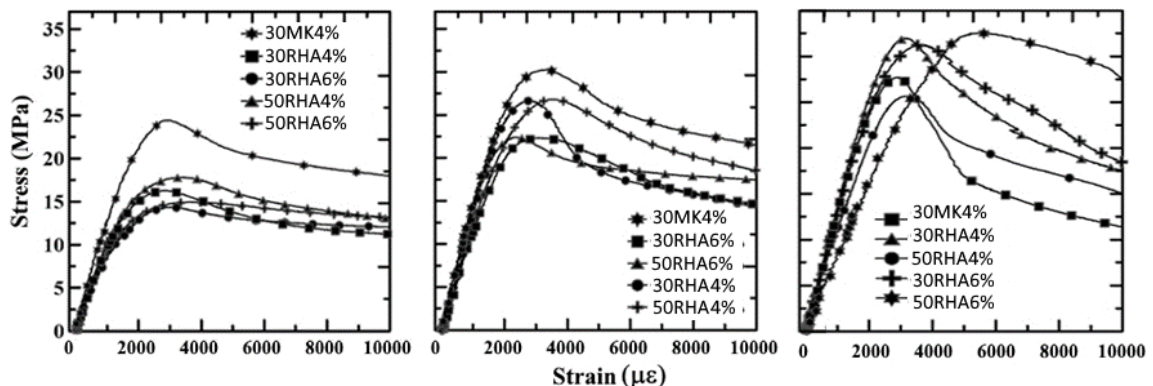


**Figure 2. Typical stress x strain curves of composites under axial compression: a) 7 days; b) 28 days; c) 56 days.**

The results presented in Table 3 demonstrate that the composites exhibited compressive strength values, at 28 days, ranging from 23.18 MPa to 29.12 MPa and modulus of elasticity values ranging from 13.68 GPa to 15.80 GPa. These mechanical properties indicate that the composites possess sufficient strength and stiffness for use in building elements without structural function.

**Table 3. Compressive strength and modulus of elasticity of composites.**

Composite	Compressive strength (MPa)			Elastic Modulus (GPa)		
	7 days	28 days	56 days	7 days	28 days	56 days
30MK4%	24.10 (0.87)	29.12 (3.41)	30.30 (5.09)	13.41 (12.40)	15.34 (3.60)	15.80 (3.23)
30RHA4%	16.08 (1.44)	25.55 (4.96)	27.69 (11.72)	11.86 (1.44)	12.21 (0.11)	14.11 (10.75)
30RHA6%	14.45 (1.10)	23.24 (5.02)	25.33(10.22)	10.32 (7.64)	11.94 (10.54)	14.02 (12.16)
50RHA4%	16.72 (8.93)	25.25 (9.88)	32.27 (9.20)	10.83 (3.34)	14.41 (6.36)	14.84 (11.36)
50RHA6%	14.69 (1.66)	23.18 (4.47)	31.64 (1.73)	9.91 (2.63)	13.11 (7.11)	13.68 (7.96)

Coefficient of variation, in % (in parentheses)

By evaluating the replacement of metakaolinite with rice husk ash, a reduction of 33.3 % and 20.4 % in compressive strength was observed at ages of 7 days and 28 days, respectively. This finding confirms the hypothesis that higher reactivity additions lead to increased mechanical strength. Specifically, for similar levels of replacement of the mineral addition with cement, using metakaolinite results in greater compressive strength than using rice husk ash at 28 days, as reported by [24].

In Fig. 3, the evolution of the compressive strength and elastic modulus of the composites is presented over a 7-day period.

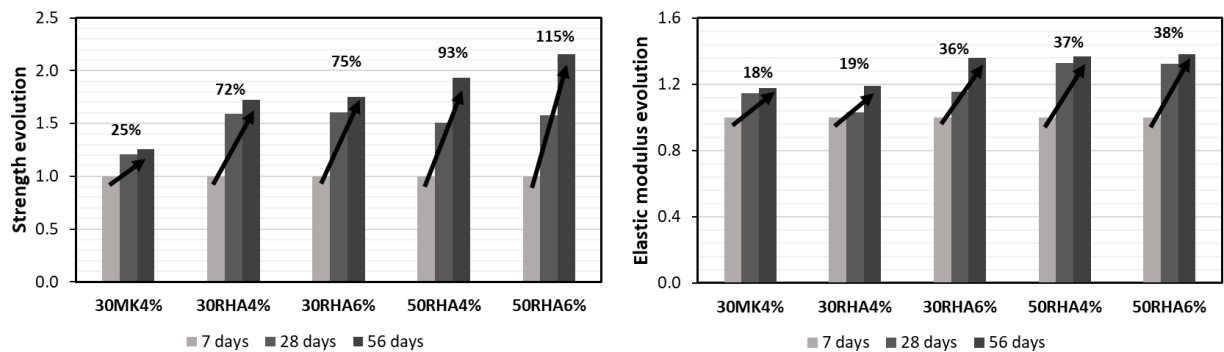


**Figure 3. Evolution of mechanical properties in relation to the 7 days of curing.**

For the 30MK4% and 30RHA4% composites, the strength evolution from 7 days to 56 days was 25 % and 72 %, respectively. However, for the 50RHA4% composite, where all mineral additions are replaced by rice husk ash, the strength evolution reached 93 % at 56 days, achieving an absolute mechanical strength greater than that of the 30MK4% composite. The strength evolution of the 50RHA composite, reaching 115 % at 56 days of age, indicates that rice husk ash exhibits slower reactivity compared to metakaolinite, which is consistent with the findings of [25]. The observed results suggest that the complete replacement of mineral additions with rice husk ash led to a favorable and continuous strength development over time.

Regarding the elastic modulus, the incorporation of rice husk ash led to a reduction in comparison to the mixtures with metakaolinite. Specifically, the reductions were 20 % and 6 % for the 30RHA4% and 50RHA4% composites, respectively, when compared to the 30MK4% composite. However, it is noteworthy that over time, specifically at an age of 56 days, the composite with 50 % rice husk ash exhibited a more significant evolution in the elastic modulus, as illustrated in Fig. 3. This indicates that the rice husk ash composite demonstrated an improved rate of stiffness development during the later stages of curing, which compensated for the initial reduction in modulus compared to the 30MK4% composite.

In general, fiber cement-based composites often experience a reduction in mechanical strength as the fiber content increases. This is attributed to the challenge of homogenizing and placing the fresh composite, especially with higher fiber volumes [26]. However, in the composites produced in this study, the increase in fiber content did not significantly impact the compressive strength at 28 days for the 30RHA and 50RHA composites. The variations in compressive strength ranged from 9.0 % to 8.2 % with a change in fiber content from 4 % to 6 % for the respective composites. Similarly, the modulus of elasticity showed minor variations, ranging from 2.2 % to 9.0 % for the same composites.

This behavior can be attributed to two factors. First, the use of a self-compacting mortar with a suitable gradation of fine content and higher superplasticizer content contributed to good workability and maintained compressive strength and modulus of elasticity even with an increase in fiber content. Second, the treatment of the fibers with calcium hydroxide contributed to the reduced water absorption of the fibers, further enhancing the overall performance of the composite [26, 29].

### 3.3.2. Flexural behavior and cracking of composites

The inclusion of fibers in cement-based composites offers significant advantages to counteract the inherent brittleness of cementitious materials under tensile stress. Fibers contribute by sustaining load capacity even after the first crack appears, allowing the composite to undergo greater deformations under direct tension or bending, resulting in enhanced ductility. Additionally, the presence of fibers significantly increases the material's energy absorption capacity, leading to improved toughness and resilience.

Fig. 4 shows the stress-displacement curves obtained for the composite containing metakaolinite. The mechanical behavior can be defined by five distinct phases [26] depending on the cracking process of the matrix. After the beginning of loading, the stress-displacement behavior of the composite is linearly elastic during Phase I, until the emergence of internal cracks in the matrix, which results in a loss of stiffness and deviation from the linearity of the stress-displacement curve. These cracks are microscopic and barely visible. With the increase in loading, there is the formation of a macrocrack, called the first visible crack, which results in an abrupt loss of tension in the composite, and which characterizes the end of Phase II. The stress in the composite at the end of Phase II is called the first crack stress ( $\sigma_{fc}$ ). After an initial abrupt drop, there is a transfer of stress between the cracked matrix and the fibers, and the stress in the composite grows again, until the appearance of a new macrocrack, which results in a new stress drop. This process, called the multiple cracking (Phase III), is influenced by fiber content and fiber-matrix adhesion.

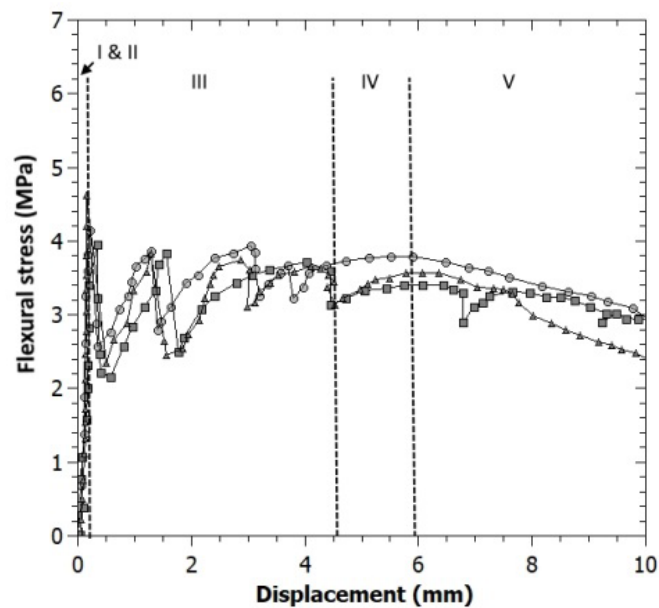


**Figure 4. Flexural behavior of composites with metakaolinite.**

Phase IV represents the end of multiple cracking, in which stress transfer in the cracked matrix is not sufficient for new cracks to appear in the matrix; the crack spacing remains constant and the increase in stress is accompanied by an increase in crack opening until coalescence of a main crack. In Phase V, the mechanical behavior of the composite is governed by the opening of this main crack. The gradual pulling out of the fibers from within the matrix in the region of the crack leads to a progressive loss of tension, and the composite's behavior becomes controlled by the frictional adhesion between the fibers and the matrix. Fig. 5 illustrates the stress-displacement curves in bending for the composites containing rice husk ash, showing a behavior similar to that observed in Fig. 4.

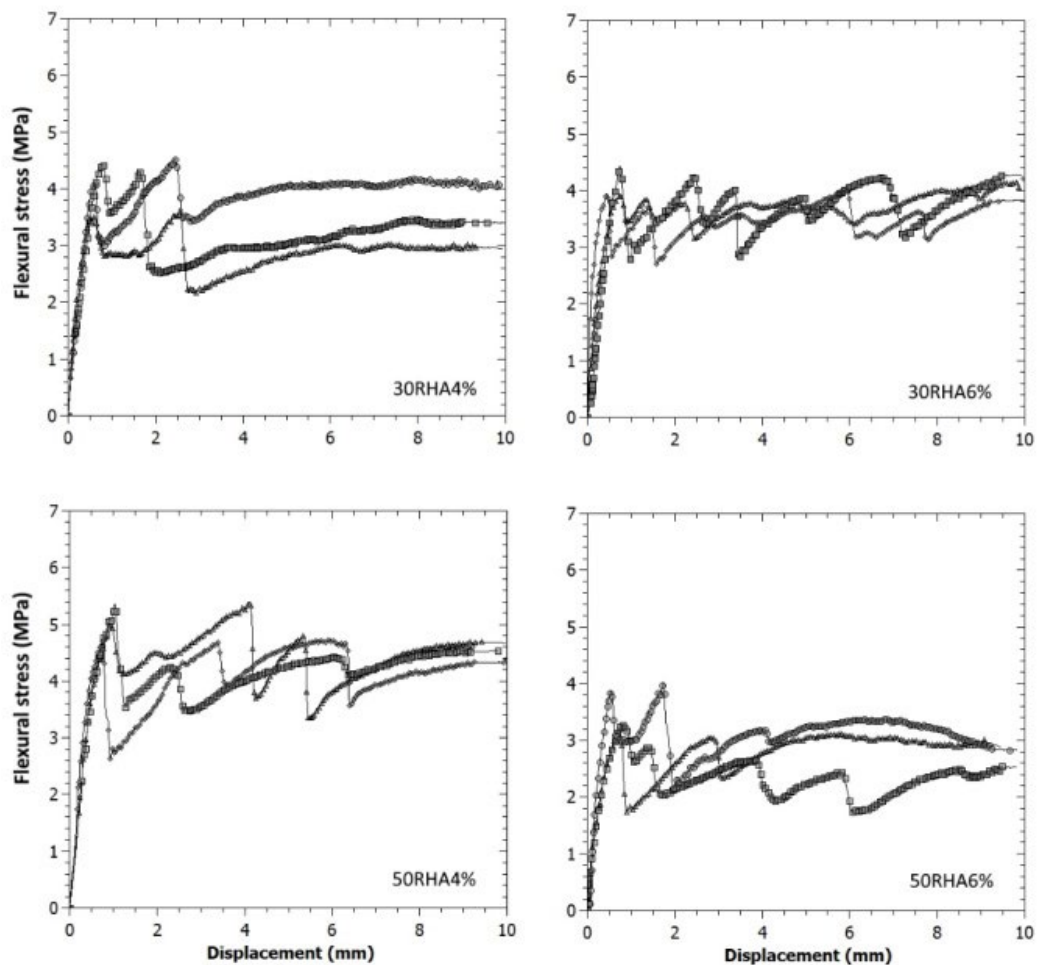
Table 6 presents the mean values and coefficients of variation in percentage (%) for the first crack stress ( $\sigma_{fc}$ ) and maximum post-cracking stress ( $\sigma_{pc}$ ) of the composite, which correspond to the highest stress level endured by the cracked composite in either Phase III or Phase IV. Additionally, the Table 6 includes the toughness, which was calculated as the area under the stress-displacement curve up to a displacement of 2 mm, equivalent to a span/150 ratio.

**Table 4. Experimental results of the four-point bending test.**

Composite	$\sigma_{fc}$ , MPa	$\sigma_{pc}$ , MPa	Toughness (N/mm)
30MK4%	4.24 (8.1)	3.88(2.0)	5.52 (6.5)
30RHA4%	4.01 (11.7)	4.15 (11.7)	6.17 (9.2)
30RHA6%	4.09 (7.1)	4.14 (3.6)	6.27 (3.8)
50RHA4%	5.02 (6.4)	4.78 (12.1)	7.03 (9.5)
50RHA6%	3.44 (10.6)	3.33 (18.50)	5.37 (14.8)

Coefficient of variation, in % (in parentheses)

Upon evaluating the replacement of metakaolinite with rice husk ash in the composites, it is verified that the 30RHA4% composite displayed a 5.4 % reduction in first crack strength compared to the 30MK4% composite, showing a proportional relationship to the reduction observed in compressive strength. For 50RHA4%, an increase of 18.4 % is verified, in relation to 30MK4%, which can be attributed to the better interaction of the matrix with the fiber and microcrack control in Phase II, which presents greater tension gain than the other composites, as shown in Fig. 5.

**Figure 5. Flexural behavior of composites with RHA.**

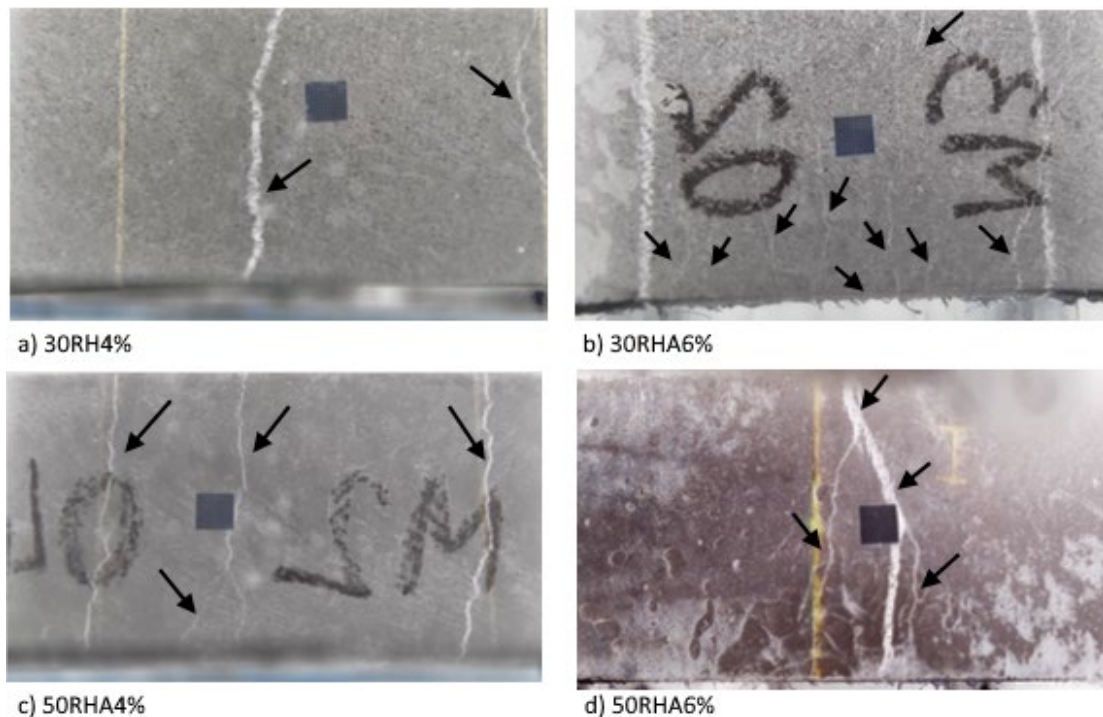
After cracking, the composites present a maximum stress that varies from 92 % to 103 % of the first crack stress, depending on the type of pozzolan and fiber content. For composites with 4 %, it appears that the use of RHA resulted in improved toughness, compared to 30MK4%. Notably, all composites demonstrated a toughness greater than 5 N/mm, indicating their superior energy absorption capacity compared to the matrix capacity of about 1.8 N/mm, with the highest toughness observed in the 50RHA4% composite. This enhanced toughness is attributed to the fibers' role in effectively transmitting stresses between cracks and, consequently, hindering the propagation of unstable cracks.

Fig. 6 presents the cracking map of the composites at 10 mm displacement, displaying the distribution of cracks and their spacing at varying fiber contents. Notably, a higher fiber content leads to a

more widespread distribution of cracks with smaller spacing between them. As the composite displacement increases, there is a notable increase in crack opening. The crack opening values range from a minimum of 0.34 mm at a displacement of 2 mm to a maximum of 1.73 mm when the displacement reaches 10 mm. It's important to note that the extent of crack opening varies based on the type of matrix and fiber content used in the composites.

Crack spacing in the composites was influenced by mineral addition and fiber content. Specifically, for the 30RHA composites, an increase in fiber content resulted in a reduction of crack spacing from 33.3 mm to 25.0 mm. However, in the 50RHA composites, the crack spacing remained constant at 25 mm for both fiber contents. Generally, smaller crack spacing indicates stronger interfacial bonding stress for composites with the same fiber content [27], underscoring its significance in understanding the composites' mechanical properties.

The behavior of the 50RHA6% composite exhibited a distinctive pattern. Instead of featuring parallel cracks, this composite demonstrated cracking characterized by the branching of small cracks around a central crack. This unusual behavior might be attributed to non-homogeneity in the distribution of fibers. Notably, this composite displayed lower workability in its fresh state, resulting in lower mechanical strength values.



**Figure 6. Crack patterns of composites with RHA.**

### 3.2. Assessment of the eco-efficiency

The results of mechanical tests indicate that, by using mineral additives to replace cement, it is possible to produce composites with appropriate mechanical strength and toughness for use in construction elements. However, with the need for sustainable building construction, it is essential that material choices are based on the environmental impact of their production. This includes considering the consumption of raw materials, energy, waste generation, and, notably, greenhouse gas emissions, known as equivalent CO<sub>2</sub> emissions (ECO<sub>2</sub>e).

Table 7 provides an overview of the materials used in composite production, including details about raw materials and primary production processes. It also presents data on ECO<sub>2</sub>e and energy (EE) consumption during material manufacturing. Conventional materials like cement and metakaolin are derived from non-renewable minerals and have substantial ECO<sub>2</sub>e and EE during their production. In the studied composites, these materials were partially or completely replaced by RHA, silica of fume, and fly ash, which are waste materials from different industrial sectors. This substitution contributes to a global effort to reduce the environmental impact of civil engineering. RHA is a byproduct of rice husk combustion for energy generation, originating from a renewable source material, and exhibits lower ECO<sub>2</sub>e and EE compared to metakaolin.

Considering the material consumption for each mix presented in Table 2, it was possible to calculate the CO<sub>2</sub> emissions and EE per volume (1 m<sup>3</sup>) of composite during production as follows:



$$ECO2e = \sum_i m_i ECO2e_i;$$

$$ECO2e = \sum_i m_i EE_i,$$

where  $ECO2e_i$  is the CO<sub>2</sub> emission equivalent per unit mass of constituent  $i$ ,  $EE_i$  is the embodied energy per unit mass of constituent  $i$  and  $m_i$  corresponds to the mass of composite ingredient  $i$  per unit volume of composite. The value adopted to calculate  $ECO2e_i$  and  $EE_i$  was the average obtained with the maximum and minimum values presented in Table 7.

**Table 5. Sustainability aspects of the materials.**

Material	Raw material		Main production operations	ECO2e (kg CO <sub>2</sub> e/ton)	EE (MJ/t)
Cement	Limestone, clay	Non-renewable	Extraction, burning, milling	750 – 1300 [17, 19, 21, 28]	3000 – 11800 [19, 29, 30]
Metakaolin	Kaolinite clay	Non-renewable	Extraction, burning, milling	236 – 840 [16, 20–22]	2720 – 3300 [18, 23]
Rice husk ash	Husk rice combustion residuals	Renewable	Grinding, drying	103.2 – 157.0 [16–17]	20 – 2070 [17–19]
Fly ash	Coal combustion residuals	Non-renewable	Grinding, drying	4 – 93 [16, 31–32]	33 – 100 [30, 32]
Silica of fume	Co-product of ferrosilicon production	Non-renewable	Grinding, drying	14 – 28 [16, 19, 21]	36 – 100 [29–30, 32]
Sand	Quartz	Non-renewable	Extraction, separation	2.4 – 13.9 [16, 19–20]	80 – 340 [29, 33]
Water	Water	Non-renewable	Extraction, treatment	0.6 – 1.3 [18–19, 29, 33]	0–200 [18–19, 29, 33]
Plasticizer	Éter policarboxilato	Non-renewable	Chemical operations	510 – 944 [29, 34]	11470 – 16260 [29–30, 35]
Natural Fiber	Vegetable plant	Renewable	Decortification, brushing, balling	182.8 – 311.0 [36–38]	4200 [38]

Fig. 7 and 8 illustrate the ECO2e and EE values for the studied composites, along with the influence of each constituent material. When replacing metakaolin (30MK4%) with rice husk ash (30RHA4%), there is a reduction of 21.0 % in ECO2e and 13.4 % in EE, indicating an increase in the sustainability of the composite. Conversely, when replacing all supplementary materials with rice husk ash (50RHA4%), there is an increase of 3.7 % and 4.3 % in ECO2e and EE, compared to the 30RHA4% mixture. This suggests that there is an increase in sustainability when using RHA in conjunction with residual supplementary materials. Nonetheless, it is important to consider that RHA is derived from a renewable plant-based source, and it has the capacity to sequester carbon during the growth of rice plants.

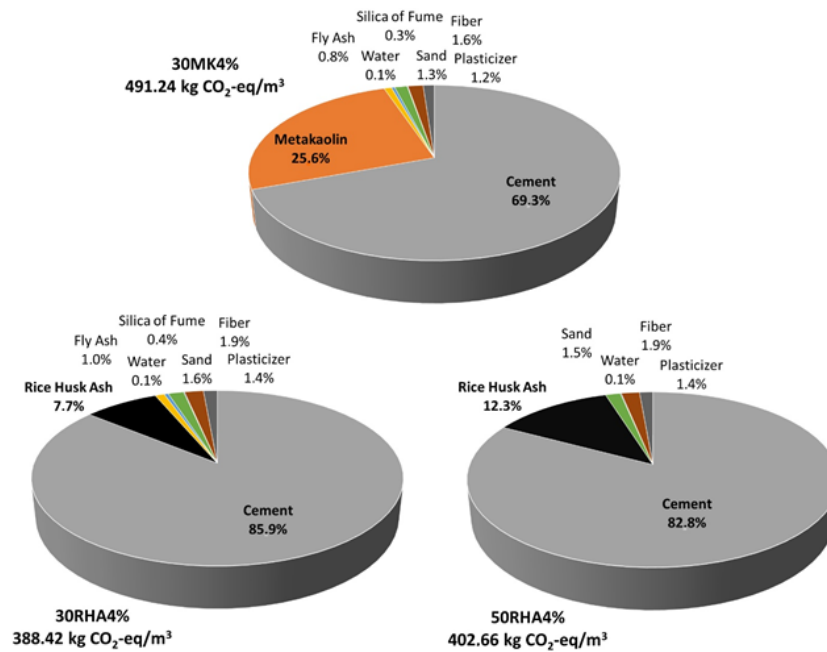


Figure 7. Emission of CO<sub>2</sub>-eq of composites reinforced with 4 % of sisal fiber.

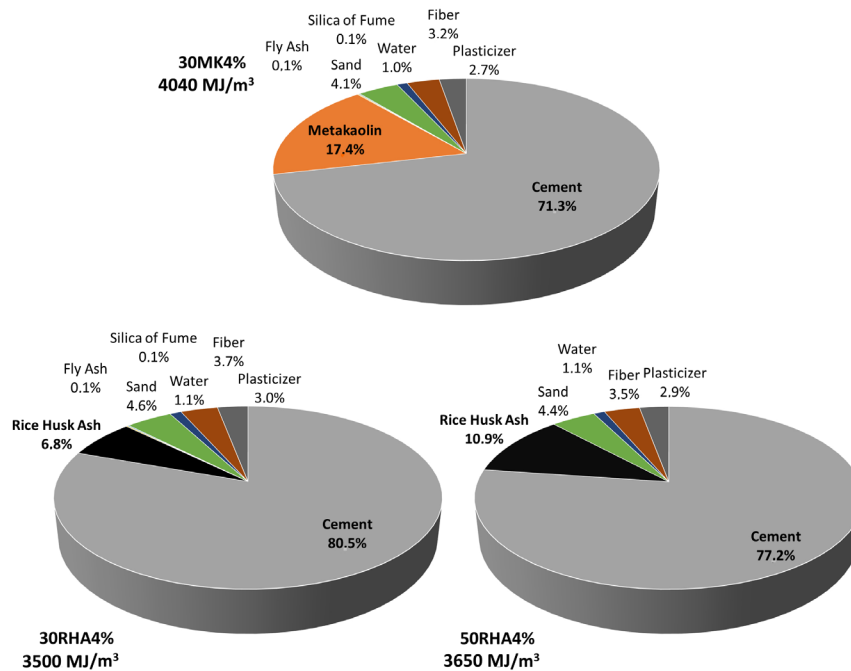


Figure 8. Embodied energy of composites reinforced with 4 % of sisal fiber.

Even though vegetable fibers originate from plants, they still require processing. Consequently, they represent the second-largest environmental impact in composite production, following the binder, despite their maximum contribution being 1.9 % to ECO<sub>2</sub>e and 3.7 % to EE. Nevertheless, the environmental impact of using vegetable fibers as reinforcement in cement matrices remains lower than that of using manufactured fibers. In the case of conventional concrete, Ali et al. [39] found that 1 % of steel fibers contributed to 36.7 % of the ECO<sub>2</sub>e in concrete. According to the authors, glass and polymeric fibers contributed 13.0 % and 4.5 %, respectively. Additionally, the emission impact of sisal fiber could be even lower if carbon sequestration during the growth of sisal plants is considered.

The evaluation of sustainability should also consider the concept of eco-efficiency, which connects the parameters ECO<sub>2</sub>e and EE with material performance indicators. As per Hasan et al. [40], this parameter is calculated using:

$$C_i = \frac{ECO_2e}{C_s}$$

where  $C_i$  represents the emission-performance efficiency and  $C_s$  is this performance requirement. According Daminieli et al. [41], in most cases  $C_s$  represents the compressive strength, but this indicator will depend of application of material. In this study,  $C_s$  was used to denote compressive strength at 7, 28, and 56 days, as well as the toughness of the composites at 28 days.

Similarly, a coefficient  $E_i$  represents the energy-performance efficiency and was established in accordance:

$$E_i = \frac{EE}{C_s}$$

Fig. 9a illustrates the emission-strength efficiency for the composites considering compressive strength. At 7 days, the mixture with metakaolin exhibits higher efficiency, as a lower  $C_i$  value corresponds to fewer ECO2e per MPa. As the hydration process of mixtures containing rice husk ash progresses slowly, there is a reduction in the  $C_i$  efficiency index. Considering the 28-day strength, which serves as a reference for the design of reinforced concrete structures, there is a reduction of 10.0 % and 5.6 % in the  $C_i$  value for the 30RHA4% and 50RHA4% mixtures, respectively, compared to the 30MK4% mixture.

The  $C_i$  values for compressive strength at 28 days ranged from 15 to 17 kg CO<sub>2</sub>e/m<sup>3</sup>-MPa, which are consistent with the values reported by Hasan et al. [42] for concrete reinforced with 4 % areca nut husk fiber, which were approximately 16.62 kg CO<sub>2</sub>e/m<sup>3</sup>-MPa. It is worth noting that the authors used a different matrix and factored in transportation emissions (30 %) in their calculations. However, it's important to highlight that the authors did not account for emissions related to the processing of the fibers, which were done manually and involved sun-drying.

The values, obtained for emission-toughness efficiency, shown in Fig. 9b, demonstrate even greater efficiency for the mixtures containing rice husk ash, with a reduction of 29.3 % and 35.7 % in the  $C_i$  value for the 30RHA4% and 50RHA4% mixtures, respectively, in comparison to the 30MK4% mixture.

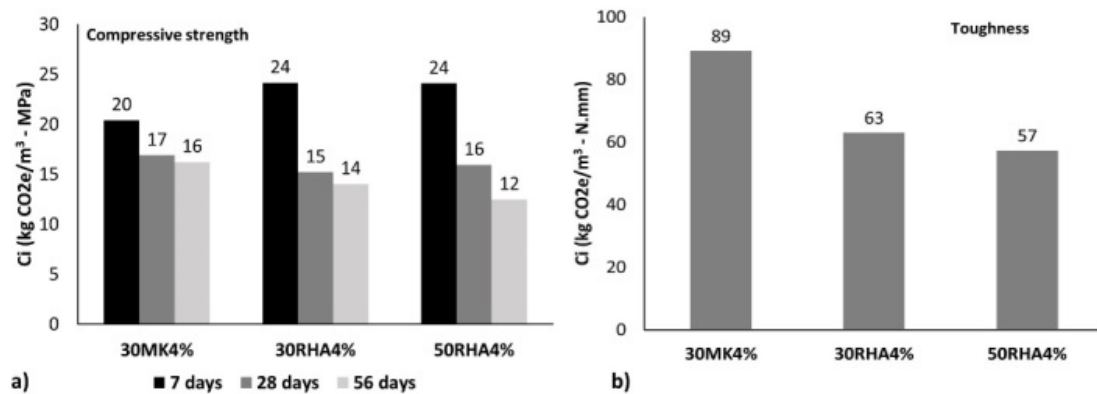


**Figure 9. Emission efficiency of composites reinforced with 4 % of sisal fibers: a) compressive strength; b) toughness.**

The energy efficiency, denoted as  $E_i$ , shown in Fig. 10, also signifies the higher sustainability of mixtures containing RHA in comparison to the mixture with metakaolin. However, when it comes to compressive strength, the best results are achieved when considering a longer hydration period. For a curing age of 56 days, the 30RHA4% and 50RHA4% mixtures exhibit reductions of 5.0 % and 15.1 %, respectively, in the  $E_i$  value compared to the 30MK4% mixture. The energy efficiency  $E_i$  concerning toughness, even at 28 days of age, shows reductions of 22.3 % and 29.0 % for the same mixtures.

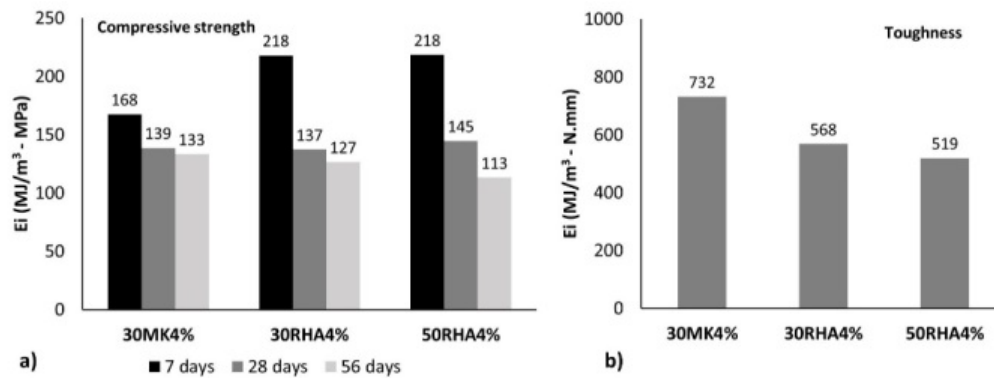


**Figure 10. Energy efficiency of composites reinforced with 4 % of sisal fibers: a) compressive strength; b) toughness.**

#### 4. Conclusions

This study examined how the composition of the cementitious matrix affects the mechanical performance and sustainability of the sisal fiber reinforced cement composites. The research primarily focused on investigating the feasibility of employing rice husk ash as an environmentally sustainable alternative to industrial mineral additives in the development of cementitious matrices for composites containing vegetable fibers.

It was verified that composites using metakaolin, which is a more reactive pozzolanic addition, exhibit higher mechanical strength and modulus of elasticity at 7 and 28 days. Composites, produced with 50 % RHA, exhibited the highest compressive strength at 56 days when compared to composites produced with metakaolin, fly ash, and silica of fume. This can be attributed to the slower reactivity of RHA in comparison to metakaolin.

Under flexural loading, SFRCC with 4 % and 6 % fiber content exhibited good post-cracking performance, with increased toughness due to a process of multiple cracking that maintained residual stress even at large deformations. The use of 50 % RHA as a substitute for cement resulted in a reduction in crack width and increased toughness.

The calculated values of CO<sub>2</sub> emissions and embodied energy per volume (1 m<sup>3</sup>) of the composite indicated that cement and metakaolin are the components with the highest environmental impact. As a result, mixtures containing RHA as a substitute for metakaolin showed a reduction of 21.0 % in CO<sub>2</sub> emissions and 13.4 % in embodied energy, indicating an increase in the sustainability of the composite. The assessment of eco-efficiency, concerning the compressive strength and toughness of the SFRCC, revealed higher efficiency in terms of CO<sub>2</sub> emissions and embodied energy consumption for the mixtures incorporating rice husk ash compared to the mixture containing metakaolin.

The incorporation of rice husk ash into cement-based composites not only improves material properties but also aligns with global initiatives to mitigate environmental impact and address climate change. This is achieved by reducing CO<sub>2</sub> emissions and embodied energy consumption compared to conventional sisal fiber-reinforced cement composites that contain metakaolinite.

#### References

- Sharifi, N.P., Jafferji, H., Reynolds, S.E., Blanchard, M.G., Sakulich, A.R. Application of lightweight aggregate and rice husk ash to incorporate phase change materials into cementitious materials. *Journal of Sustainable Cement-Based Materials*. 2016. 5(6). Pp. 349–369. DOI: 10.1080/21650373.2016.1207576
- Ahsan, M.B., Hossain, Z. Supplemental use of rice husk ash (RHA) as a cementitious material in concrete industry. *Construction and Building Materials*. 2018. 178. Pp. 1–9. DOI: 10.1016/j.conbuildmat.2018.05.101
- Ling, I.H., Teo, D.C.L. Properties of EPS RHA lightweight concrete bricks under different curing conditions. *Construction and Building Materials*. 2011. 25. Pp. 3648–3655. DOI: 10.1016/j.conbuildmat.2011.03.061
- Liu, C., Zhang, W., Liu, H., Zhu, C., Wu, Y., He, C., Wang, Z. Recycled aggregate concrete with the incorporation of rice husk ash: Mechanical properties and microstructure. *Construction and Building Materials*. 2022. 351. Article no. 128934. DOI: 10.1016/j.conbuildmat.2022.128934
- Kannur, B., Chore, H.S. Low-fines self-consolidating concrete using rice husk ash for road pavement: An environment-friendly and sustainable approach. *Construction and Building Materials*. 2023. 365. Article no. 130036. DOI: 10.1016/j.conbuildmat.2022.130036
- Ranasinghe, A. Rice husk and rice straw ashes can prevent cracks in natural fibre reinforced concrete roofing elements. *Engineer*. 1986. 14. Pp. 9–32.
- Gram, H.E., Nimityongskul, P. Durability of natural fibres in cement-based roofing sheets. *Journal of Ferrocement*. 1987. 17(4). Pp. 321–327.

8. Shafiq, N., Robles-Austriaco, L., Nimityongskul, P. Durability of natural fibers in RHA mortar. *Journal of Ferrocement*. Journal of Ferrocement. 1988. 18(3). Pp. 249–262.
9. Lima, P.R.L., Barros, J.A., Roque, A.B., Fontes, C.M., Lima, J.M. Short sisal fiber reinforced recycled concrete block for one-way precast concrete slabs. *Construction and Building Materials*. 2018. 187. Pp. 620–634. DOI: 10.1016/j.conbuildmat.2018.07.184
10. Frazão, C., Barros, J.A., Toledo Filho, R.D., Ferreira, S., Gonçalves, D. Development of sandwich panels combining sisal fiber-cement composites and fiber-reinforced lightweight concrete. *Cement and Concrete Composites*. 2018. 86. Pp. 206–223. DOI: 10.1016/j.cemconcomp.2017.11.008
11. Tonoli, G.H.D., Santos, S.F.D., Rabi, J.A., Santos, W.N.D., Savastano Junior, H. Thermal performance of sisal fiber-cement roofing tiles for rural constructions. *Scientia Agricola*. 2011. 68. Pp. 1–7. DOI: 10.1590/S0103-90162011000100001
12. Feng, S., Lyu, J., Xiao, H., Feng, J. Application of cellulose fibre in ultra-high-performance concrete to mitigate autogenous shrinkage. *Journal of Sustainable Cement-Based Materials*. 2023. 12(7). Pp. 842–855. DOI: 10.1080/21650373.2022.2119618
13. Ezugwu, E.K., Calabria-Holley, J., Paine, K. Physico-mechanical and morphological behavior of hydrothermally treated plant fibers in cementitious composites. *Industrial Crops and Products*. 2023. 200. Article no. 116832. DOI: 10.1016/j.indcrop.2023.116832
14. Toledo Filho, R.D., Ghavami, K., England, G.L., Scrivener, K. Development of vegetable fibre–mortar composites of improved durability. *Cement and Concrete Composites*. 2003. 25(2). Pp. 185–196. DOI: 10.1016/S0958-9465(02)00018-5
15. Wei, J., Meyer, C. Utilization of rice husk ash in green natural fiber-reinforced cement composites: Mitigating degradation of sisal fiber. *Cement and Research*. 2016. 81. Pp. 94–111. DOI: 10.1016/J.CEMCONRES.2015.12.001
16. Ozturk, E., Ince, C., Derogar, S., Ball, R. Factors affecting the CO<sub>2</sub> emissions, cost efficiency and eco-strength efficiency of concrete containing rice husk ash: A database study. *Construction and Building Materials*. 2022. 326. Article no. 126905. DOI: 10.1016/J.CONBUILDMAT.2022.126905
17. Hu, L., He, Z., Zhang, S. Sustainable use of rice husk ash in cement-based materials: Environmental evaluation and performance improvement. *Journal of Cleaner Production*. 2020. 264. Article no. 121744. DOI: 10.1016/J.JCLEPRO.2020.121744
18. Arrigoni, A., Panesar, D.K., Duhamel, M., Opher, T., Saxe, S., Posen, I.D., MacLean, H.L. Life cycle greenhouse gas emissions of concrete containing supplementary cementitious materials: cut-off vs. substitution. *Journal of Cleaner Production*. 2020. 263. Article no. 121465. DOI: 10.1016/J.JCLEPRO.2020.121465
19. Selvaranjan, K., Navaratnam, S., Gamage, J.C.P.H., Thamboo, J., Siddique, R., Zhang, J., Zhang, G. Thermal and environmental impact analysis of rice husk ash-based mortar as insulating wall plaster. *Construction and Building Materials*. 2021. 283. Article no. 122744. DOI: 10.1016/J.CONBUILDMAT.2021.122744
20. Chandar, S.P., Raganathan, S., Ramachandran, R. CO<sub>2</sub> emission analysis of metakaolin and alccofine replaced cement in M40 grade concrete. *Environmental Science and Pollution Research*. 2023. 30(47). Pp. 104408–104414. DOI: 10.1007/s11356-023-29771-4
21. Maddalena, R., Roberts, J.J., Hamilton, A. Can Portland cement be replaced by low-carbon alternative materials? A study on the thermal properties and carbon emissions of innovative cements. *Journal of Cleaner Production*. 2018. 186. Pp. 933–942. DOI: 10.1016/J.JCLEPRO.2018.02.138
22. Asghari, Y., Mohammadyan-Yasouj, S.E., Kolor, S.S.R. Utilization of metakaolin on the properties of self-consolidating concrete: A review. *Construction and Building Materials*. 2023. 389. Article no. 131605. DOI: 10.1016/J.CONBUILDMAT.2023.131605
23. Tasiopoulou, T., Katsourinis, D., Giannopoulos, D., Founti, M. Production-Process Simulation and Life-Cycle Assessment of Metakaolin as Supplementary Cementitious Material. *Eng*. 2023. 4(1). Pp. 761–779. DOI: 10.3390/ENG4010046
24. Kannan, V., Ganesan, K. Chloride and chemical resistance of self compacting concrete containing rice husk ash and metakaolin. *Construction and Building Materials*. 2014. 51. Pp. 225–234. DOI: 10.1016/J.CONBUILDMAT.2013.10.050
25. Langaro, E.A., Santos, C.A. dos, Medeiros, M.H.F., Jesus, D.S., Pereira, E. Rice husk ash as supplementary cementing material to inhibit the alkali-silica reaction in mortars. *Revista IBRACON de Estruturas e Materiais*. 2021. 14(4). Article no. e14404. DOI: 10.1590/S1983-41952021000400004
26. Silva, F.A., Mobasher, B., Toledo Filho, R.D. Cracking mechanisms in durable sisal fiber reinforced cement composites. *Cement and Concrete Composites*. 2009. 31(10). Pp. 721–730. DOI: 10.1016/J.CEMCONCOMP.2009.07.004
27. Mobasher, B., Peled, A., Pahilajani, J. Distributed cracking and stiffness degradation in fabric-cement composites. *Materials and Structures*. 2006. 39(3). Pp. 317–331. DOI: 10.1007/S11527-005-9005-8
28. Josa, A., Aguado, A., Heino, A., Byars, E., Cardim, A. Comparative analysis of available life cycle inventories of cement in the EU. *Cement and Concrete Research*. 2004. 34(8). Pp. 1313–1320. DOI: 10.1016/J.CEMCONRES.2003.12.020
29. Yu, J., Lu, C., Leung, C.K.Y., Li, G. Mechanical properties of green structural concrete with ultrahigh-volume fly ash. *Construction and Building Materials*. 2017. 147. Pp. 510–518. DOI: 10.1016/J.CONBUILDMAT.2017.04.188
30. Jones, R., McCarthy, M., Newlands, M. Fly ash route to low embodied CO<sub>2</sub> and implications for concrete construction. *Proceedings of World of Coal Ash (WOCA) Conference*. Denver. 2011. Pp. 1–14.
31. Han, Y., Lin, R.S., Wang, X.Y. Compressive Strength Estimation and CO<sub>2</sub> Reduction Design of Fly Ash Composite Concrete. *Buildings*. 2022. 12(2). Pp. 139. DOI: 10.3390/BUILDINGS12020139
32. Hammond, G.P., Jones, C.I. Embodied energy and carbon in construction materials. *Proceedings of the Institution of Civil Engineers-Energy*. 2008. 161(2). Pp. 87–98. DOI: 10.1680/ENER.2008.161.2.87
33. Long, W.J., Li, H.D., Wei, J.J., Xing, F., Han, N. Sustainable use of recycled crumb rubbers in eco-friendly alkali activated slag mortar: Dynamic mechanical properties. *Journal of Cleaner Production*. 2018. 204. Pp. 1004–1015. DOI: 10.1016/J.JCLEPRO.2018.08.306
34. Zhang, Y.R., Liu, M.H., Xie, H.B., Wang, Y.F. Assessment of CO<sub>2</sub> emissions and cost in fly ash concrete. *Proceedings of the 2014 3<sup>rd</sup> International Conference on Frontier of Energy and Environment Engineering*. Taiwan, 2014. Pp. 327–331.
35. Zheng, H. Concrete for Sustainability. [Online] System requirements: AdobeAcrobatReader. URL: [https://www.devb.gov.hk/filemanager/en/content\\_680/7\\_dr\\_herbert\\_zheng\\_concrete\\_for\\_sustainability.pdf](https://www.devb.gov.hk/filemanager/en/content_680/7_dr_herbert_zheng_concrete_for_sustainability.pdf) (date of application: 26.01.2024)
36. De Beus, N., Carus, M., Barth, M. Carbon Footprint and Sustainability of Different Natural Fibres for Biocomposites and Insulation Material. 2019, Accessed: Jan. 23, 2024. [Online]. Available: [www.nova-institut.eu](http://www.nova-institut.eu)

37. Dellaert, S.N.C. Sustainability assessment of the production of sisal fiber in Brazil. 2014, Accessed: Jan. 23, 2024. [Online]. Available: <https://studenttheses.uu.nl/handle/20.500.12932/17383>
38. Broeren, M.L.M., Dellaert, S.N.C., Cok, B., Patel, M.K., Worrell, E., Shen, L. Life cycle assessment of sisal fibre – Exploring how local practices can influence environmental performance. *Journal of Cleaner Production*. 2017. 149. Pp. 818–827. DOI: 10.1016/J.JCLEPRO.2017.02.073
39. Ali, B., Qureshi, L.A., Kurda, R. Environmental and economic benefits of steel, glass, and polypropylene fiber reinforced cement composite application in jointed plain concrete pavement. *Composites Communications*. 2020. 22. Article no. 100437. DOI: 10.1016/J.COCO.2020.100437
40. Hasan, N.M.S., Shaurdho, N.M.N., Sobuz, M.H.R., Meraz, M.M., Basit, M.A., Paul, S.C., Miah, M.J. Rheological, Mechanical, and Micro-Structural Property Assessment of Eco-Friendly Concrete Reinforced with Waste Areca Nut Husk Fiber. *Sustainability*. 2023. 15(19). Article no. 14131. DOI: 10.3390/SU151914131
41. Damineli, B.L., Kemeid, F.M., Aguiar, P.S., John, V.M. Measuring the eco-efficiency of cement use. *Cement and Concrete Composites*. 2010. 32(8). Pp. 555–562. DOI: 10.1016/J.CEMCONCOMP.2010.07.009

**Contacts:**

**Kaline Guerra Calazans,**

ORCID: <https://orcid.org/0000-0002-4963-6216>

E-mail: [kaline.guerracalazans@hotmail.com](mailto:kaline.guerracalazans@hotmail.com)

**Paulo Roberto Lopes Lima,**

ORCID: <https://orcid.org/0000-0003-2937-9520>

E-mail: [prllima@uefs.br](mailto:prllima@uefs.br)

**Romildo Dias Toledo Filho,**

ORCID: <https://orcid.org/0000-0001-5867-4452>

E-mail: [toledo@coc.ufrj.br](mailto:toledo@coc.ufrj.br)

*Received 29.01.2024. Approved after reviewing 27.02.2024. Accepted 28.02.2024.*